

# **GEOCHEMICAL ASSESSMENT OF THE MT. CAMIGUIN DE BABUYANES GEOTHERMAL FIELD, CALAYAN, CAGAYAN, PHILIPPINES**

**Rizabigail G. Reyes**  
Department of Energy  
Energy Center, Rizal Drive cor. 34<sup>th</sup> Street  
Bonifacio Global City, Taguig City  
PHILIPPINES  
*rgreyes@doe.gov.ph*

## **ABSTRACT**

The geothermal and non-geothermal water chemistry associated with the Camiguin de Babuyanesis Geothermal Field was studied. The aim was to characterize the water, estimate the temperature of the reservoir and propose geothermal utilization. The waters are alkali-chloride, sulphate chloride and bicarbonate waters. No sampled thermal waters are representatives of the deep geothermal system below. Instead, they are likely to represent a mixture of deep geothermal waters with seawater or shallow groundwaters. The chalcedony geothermometer indicates that the minimum temperature of the reservoir is 97-167°C. Based on the chemical composition and temperature, these waters are suitable for direct use and binary power generation. Calcite scaling is expected and amorphous silica when waters cool down.

## **1. INTRODUCTION**

The Philippines is ranked the third largest power producer of geothermal energy next to the United States of America and Indonesia with 1928 MW installed capacity (Fronza et al., 2021). The latest resource estimation for the geothermal energy potential in the country is 4064 MW with a total of 82 geothermal areas, 7 of which are producing fields, 18 are under exploration by private companies and 57 areas are open for exploration (Fronza et al., 2021). To increase the capacity of the country, the Philippines Department of Energy (DOE) started resource assessment projects in 2011. To date, a total of 12 areas were explored through locally funded projects (LFP). One of DOE's LFPs is the Comprehensive Resource Assessment of Philippine Low-Enthalpy Geothermal Areas (CRAPLEGA), implemented from January 2015 to December 2017. Three geothermal areas were selected for geological, geochemical, and geophysical surveys. The project was then awarded to Diamond Drilling Corporation of the Philippines.

One of the geothermal areas under the above project is Camiguin de Babuyanesis, located on the northernmost part of the Philippines (Figure 1). Geochemical data from the 2015 and 2016 surveys were used in this study to re-evaluate the geothermal potential of the island. The specific objectives are the following: to estimate the reservoir temperature of the geothermal system, to determine the chemistry of the reservoir fluid, to classify the types of water present in the area and to identify the processes that affects the fluid during its transport from the reservoir to the surface.

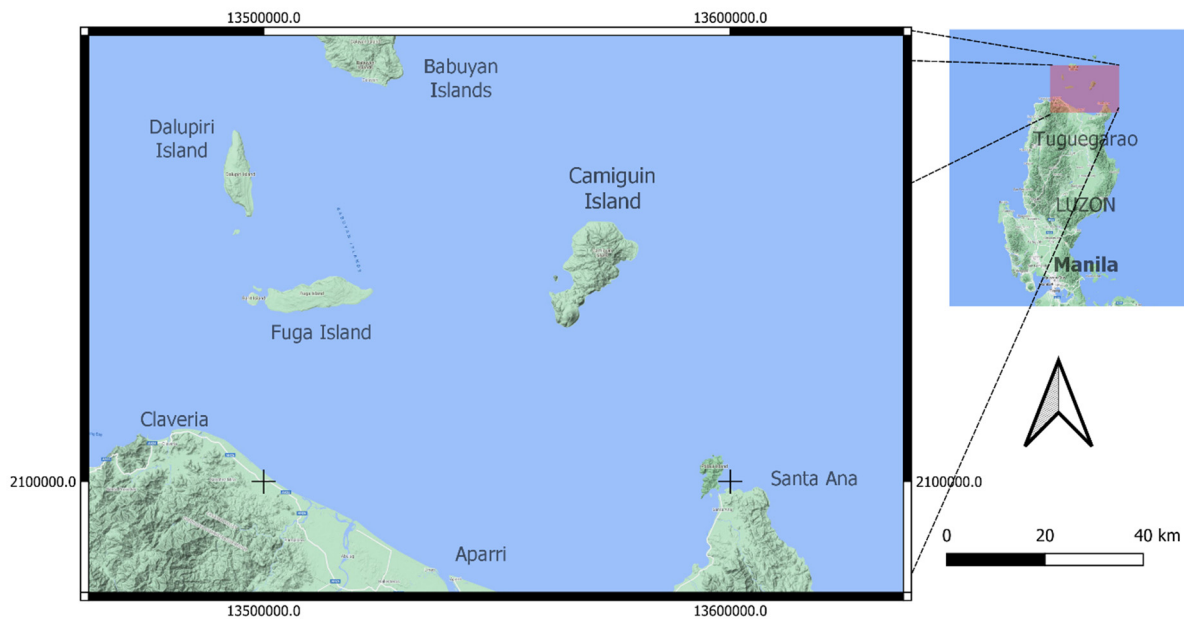


FIGURE 1: Location map of Camiguin de Babuyanes

## 2. GEOLOGY OF THE STUDY AREA

Camiguin de Babuyanes Island has four volcanic centres: Mt. Camiguin, Mt. Malabsing, Pamoctan and Didicas volcano. The northern part of the island is composed of a calc-alkaline andesite shield volcano with effusive events and alternating lava and pyroclastic flows. It is dated to the Mio-Pliocene (3-7 Ma); (Peña and Aurelio, 2010). Detailed information on the regional geology and tectonic settings can be found in Appendix I.

The result of the geological survey under CRAPLEGA is summarized below. Based on the 2015 survey (Figure 2), the lithology of the island is limestone, older alternating andesite and pyroclastics, younger andesite and pyroclastic (tuff, tuffaceous sediments, agglomerate) alternation, bioherm deposits and alluvium (Department of Energy, 2017).

The oldest rock in the area is limestone and is dated to the Plio-Pleistocene based on the red algae, echinoid spine (sp.), amphistagina sp., operculina sp., milliloid lithoclasts and corals. It is distributed along the northern coastline of the island (Department of Energy, 2017).

Widespread on the central and northern part of the island are the older alternating andesite and pyroclastics dated to the Pleistocene-Quaternary (Figure 2). Some of the outcrops are altered but no hot springs were observed, indicating that the altered grounds are relicts. The andesites are massive and occur in lava form exhibiting sheeting and columnar jointing. The colour of the rock samples is grey to brown and has porphyritic texture showing feldspar and hornblende crystals. The older pyroclastic is dipping 30-40° (Department of Energy, 2017).

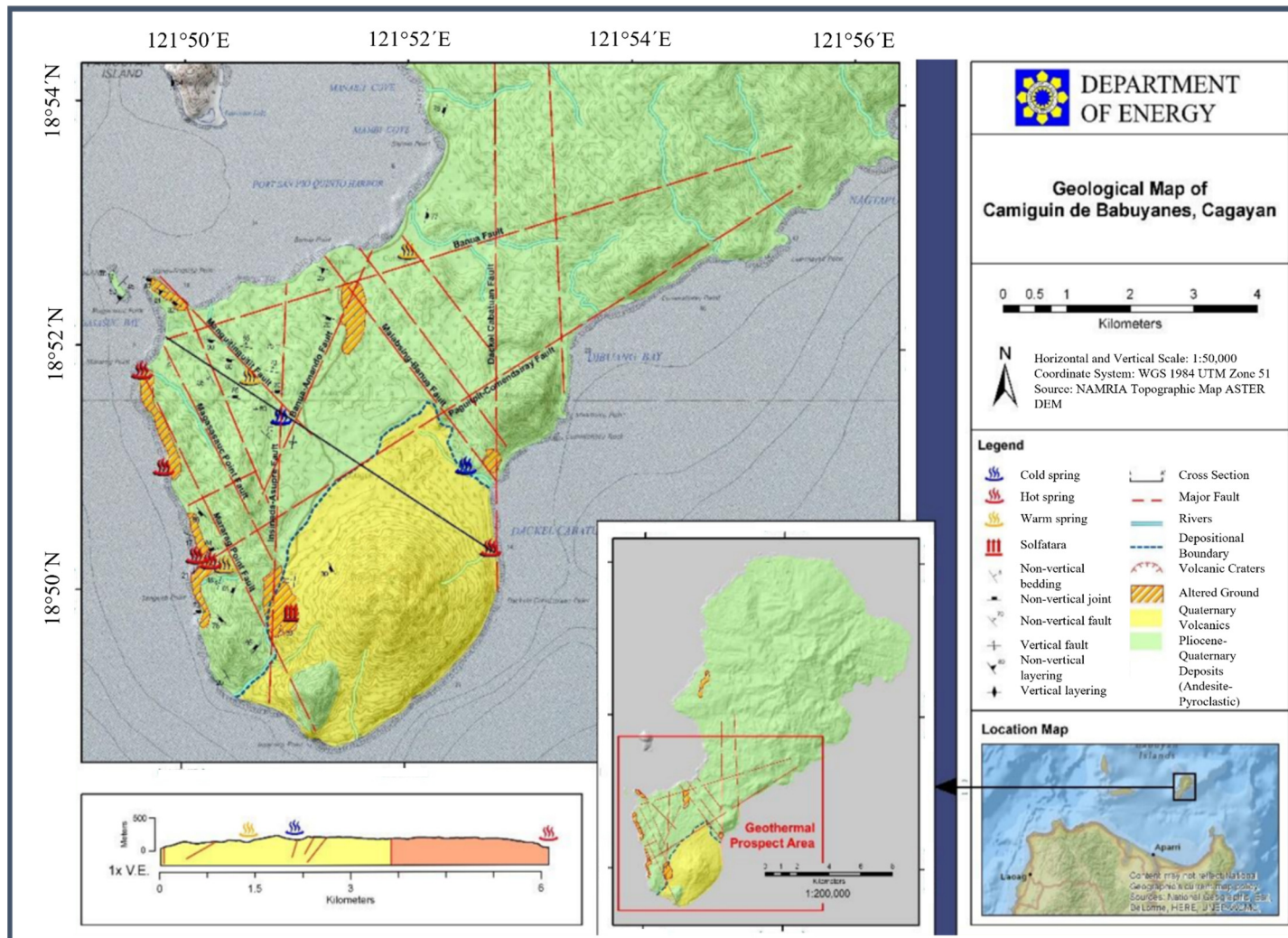


FIGURE 2: Geological map of southern area of Camiguin de Babuyanes (Department of Energy, 2017)

On the southern part of the island and around the Mt. Camiguin volcano, younger andesite and pyroclastics (tuff, tuffaceous sediments, agglomerate) alternation (Figure 2) were mapped. These andesites are not altered. The pyroclastics are low dipping ( $5\text{-}15^\circ$ ) to almost horizontal and dip radially away from the volcanic centre. These are also widely distributed on the southern part of the island (Department of Energy, 2017).

Bioherm deposits were observed along the coastline of Magasasuc. They are white, fresh, and indurated. The trend of the beds is  $N5^\circ E$  to  $N5^\circ W$  and has a low dip. A variety of marine invertebrates like corals were cemented by calcareous materials (Department of Energy, 2017).

The youngest deposit in the area is an alluvium. It is distributed along the coastline, along Karayan River of Balatubat and Mangitingit Creek of Naguilian. It is composed of unconsolidated sand to boulder sized sediments which are andesitic in composition (Department of Energy, 2017).

### 3. METHODOLOGY

#### 3.1 Field sampling

The water samples for this study were collected in 2015 and 2016. Three samples (1 hot spring, 1 cold spring and seawater) were taken 06-13 May 2015 as part of a reconnaissance survey. A detailed survey was conducted 04-08 April 2016 and nine manifestations (4 hot springs, 1 warm spring, 4 background samples) were sampled. An additional two warm spring samples were taken on 18 May 2016. All sampling locations are shown in Figure 3.

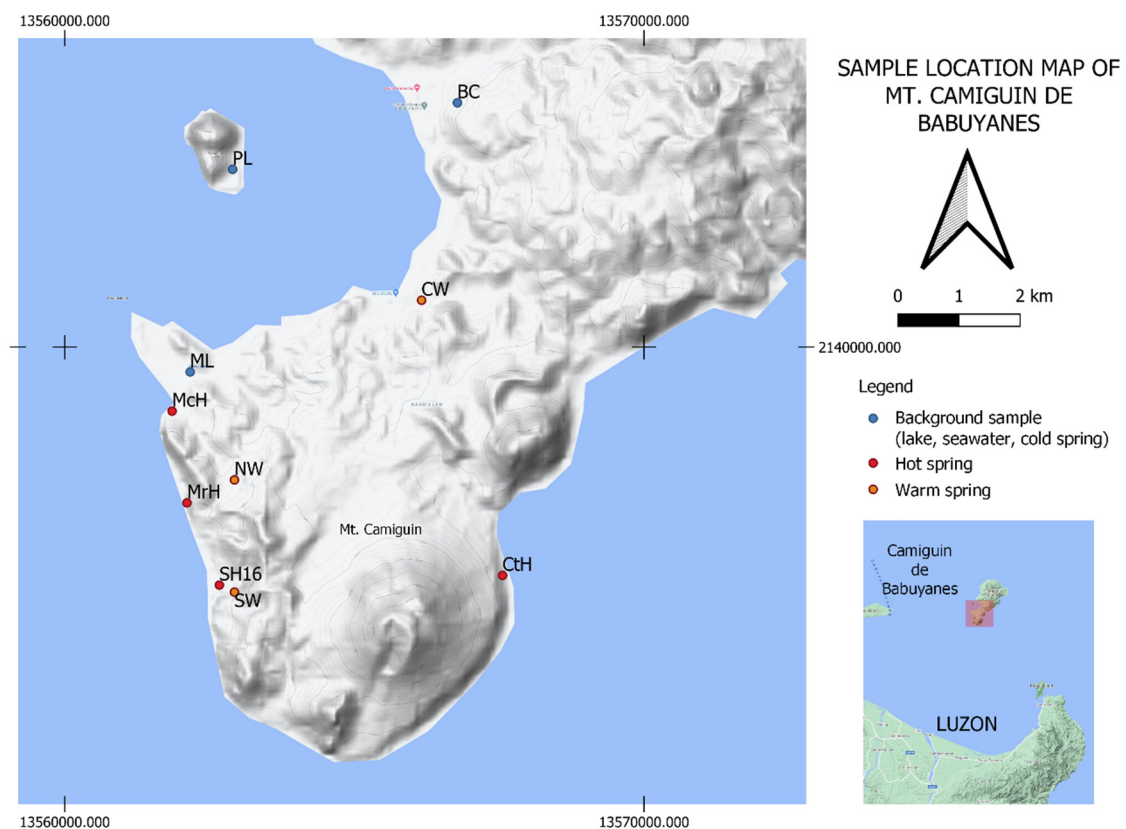


FIGURE 3: Camiguin De Babuyanes sample location map

Temperature, pH, and flow rate were measured *in situ* at each location. Four water samples were taken from each site (Figure 4) and labelled accordingly. The label for the bottles includes the date (year, month, day), spring name (CDB-HS/WS/CS #), pH and temperature.

Temperatures and pH were recorded on site using a dial thermometer, pH-temperature multimeter and pH indicator strips. Samples for major anions were collected into plastic bottles without any treatment, whereas samples for major cations were filtered using 0.45  $\mu\text{m}$  Millipore filter and acidified using nitric acid (Table 1). Samples for alkalinity test were collected into air-tight amber glass bottles to avoid air contamination. The flow rate (Figure 5) was estimated by measuring three times the time needed for a leaf to travel one metre distance along the flow channel multiplied by the cross section, estimated from the length, width, and depth of the channel.



FIGURE 4: Pictures of one set of samples



FIGURE 5: Flow rate determination

### 3.2 Chemical analysis

The samples were analysed at the laboratory of the Philippines DOE. The analytical methods used in this study are summarized in Table 1. The major anions were analysed using titrimetry and colorimetry respectively for Cl and SO<sub>4</sub>. The HCO<sub>3</sub> was analysed using the potentiometric method. The cations were measured using atomic absorption spectrophotometry (AAS). The analytical uncertainty estimated from the charge balance is 0.2-24%.

TABLE 1: Sample treatment for the various water analyses done in the field

Container	Sample treatment	Analysis	Method	Laboratory
500 ml polyethylene plastic bottle	Raw, unfiltered and unacidified	Chloride, sulphate	Chloride – Titrimetric Sulphate – Colorimetric	Philippines Department of Energy
500 ml polyethylene plastic bottle	Filtered using a 0.45 $\mu\text{m}$ Millipore filter and acidified with nitric acid	Si, Na, K, Ca, Mg, Fe, Rb, Li, Cs	Atomic Absorption Spectrophotometry	
350 ml glass bottle with latex rubber tubing and tightly clamped to prevent air contamination		Air-free, unfiltered and unacidified	alkalinity test (pH, B, HCO <sub>3</sub> )	pH – electrometric B, HCO <sub>3</sub> – Potentiometric

### 3.3 Geochemical calculations

The computer program WATCH 2.4 was used to reconstruct the deep fluid pH, chemical composition, and temperature based on the discharge chemistry of the samples collected in this study (Arnórsson et al. 1982, Bjarnason 2010). The chalcedony, quartz, and Na/K geothermometers were used to assess the deep aquifer temperature (Fournier and Potter, 1982; Fournier, 1977; Arnórsson et al., 1983). Detailed information regarding the WATCH program can be found in Arnórsson et al. (1982) and Bjarnason (2010).

The changes of the chemical composition during the ascent of the deep fluid to the surface were modelled using an adiabatic boiling and a conductive cooling model. The boiling model assumes that boiling has occurred but there is no change in heat or mass of the rising fluid from the reservoir to the surface. This process causes changes in the composition of the rising geothermal fluid due to decrease in temperature and mineral dissolution or precipitation (Arnórsson et al, 2007) Conductive cooling assumes that heat loss occurs as the geothermal fluid rises through cooler rocks or by boiling caused by decreasing hydrostatic head (Arnórsson et al, 2007)

The speciation and saturation state of the fluids with respect to chosen mineral phases were also assessed using PHREEQC Interactive v.3.3.9 (Parkhurst and Apello, 2013) with the *carbfix.dat* thermodynamic database (Voigt et al., 2018). The mineral saturation state of the fluid at various temperatures calculated by PHREEQC were then used to create multiple mineral equilibria plots to verify the chosen geothermometer. The saturation index SI of each mineral can be defined as  $\log(Q/K)$ , where K is the equilibrium constant and Q the ion activity product. It is a measure of the proximity of the aqueous solution to equilibrium with a mineral (Reed and Spycher, 1984). The plot of SI or  $\log(Q/K)$  as a function of temperature can provide information if the water is in equilibrium with a host rock mineral assemblage, identify probable mineral assemblages as well as the temperature of equilibrium (Reed and Spycher, 1984).

The liquid analysis spreadsheet ver. 3 from Powell and Cumming (2010) was also used to compare the subsurface temperature with the WATCH geothermometers. This spreadsheet uses mathematical formulas to calculate various geothermometers in addition to geothermometers in WATCH, e.g., amorphous silica, alpha cristobalite, beta cristobalite, Na-K-Ca, Na/K (Fournier, 1979; Truesdell, 1976; Giggenbach, 1988; Tonani, 1980; Nieva and Nieva, 1987; K/Mg Giggenbach, 1988). In addition, it creates ternary plots and graphs for water classification. This classification is helpful to evaluate the origin and processes that dictate the chemical composition of geothermal waters. The charts included are the Giggenbach Na-K-Mg geothermometer ternary diagram, three temperature “geoindicator” cross-plots,  $\delta^{18}\text{O}$ -  $\delta\text{D}$ , Cl-enthalpy and four commonly traced element ternary plots. Further information can be found in Powell and Cumming (2010).

## 4. RESULTS AND DISCUSSION

### 4.1 Water chemistry

#### 4.1.1 Description of waters (surface, groundwater and thermal)

The result of the analysis for the Camiguin de Babuyan hot and warm springs, cold spring, cold well, seawater and lake waters are presented in Table 2. The sampling temperature of seawater (S5 and S6), Lake Magasasuc (McL) and Lake Pamoctan (PL) is close to ambient from 28.2-35.8°C. The pH ranges from 5.2 to 9.02. The dominant cation for the lake waters is Na and the dominant anion is Cl. For the seawater, the dominant cations are Na and Mg with considerable amounts of K and Ca while the dominant anions are Cl and  $\text{SO}_4$ . Boron is not detected for McL, it is, however, 7.88 ppm for PL. Boron concentrations for seawater range from 4.9-11 ppm.

TABLE 2. Chemical composition of the water samples

Sample ID	Date	T	pH	pH-T	B	HCO <sub>3</sub>	Cl	Ca	Na	Mg	K	SiO <sub>2</sub>	SO <sub>4</sub>	Cs	Fe	Rb	Li	IB		
		°C		°C	ppm	ppm	ppm	ppm	ppm	ppm	ppm	ppm	ppm	ppm	ppm	ppm	ppm	c	d	e
SH5	05.2015	90	2.02	25.6	12.7	a	2100	213	931	84.9	92.3	184	1780	0.32	6.51	0.51	1.26	-24.2	-15.6	-12.7
SH6	02.04.2016	89.6	1.53	<sup>b</sup> 22.2	14.3	a	1870	224	937	92.9	94.6	181	1860	0.18	6.67	0.5	1.3	19.2	0.1	9.2
MrH	02.04.2016	63.9	2.57	<sup>b</sup> 22.2	5.89	a	2390	143	1310	130	68.2	68.9	617	0.12	0.35	0.29	0.78	0.2	-0.6	-0.4
CtH	03.04.2016	86.8	7.93	<sup>b</sup> 22.2	2.95	272	733	69.9	482	46	57.1	259	306	<0.1	0.05	0.17	0.33	-11.6	-2.9	-2.0
McH	06.04.2016	86.5	7.05	<sup>b</sup> 22.2	7.35	337	5510	416	3130	267	209	81.5	767	0.19	0.75	0.53	2.03	3.4	2.1	1.7
CW	03.04.2016	39.9	8.76	<sup>b</sup> 22.2	ND	158	71.1	32.5	61.6	16.3	12.3	99.1	19.9	ND	0.05	0.04	<0.02	-6.0	8.7	-10.1
SW	18.04.2016	40	7.12	23.0	<1	116	90	46.5	59.2	19.2	4.05	107	94.7	<0.1	0	<0.05	<0.02	-3.3	1.3	0.8
NW	18.04.2016	42	6.98	24.1	ND	62.2	71.8	41.6	53	14.2	4.1	101	127	<0.1	0	<0.05	ND	-3.3	-0.3	-10.2
SC	05.2015	30	7.07	25.7	1.22	94.5	89	38.2	63.9	16.3	3.98	93.7	114	0.34	0.25	<0.05	ND	-9.4	-2.4	11.8
BC	04.04.2016	26.7	7.29	<sup>b</sup> 22.2	ND	99.4	23	21.3	24.5	7.37	2.32	73.7	6.72	<0.1	0.45	<0.02	ND	-0.6	7.5	-47.2
McL	02.04.2016	35.8	9.02	<sup>b</sup> 22.2	ND	ND	1200	19.6	712	46	24.5	3.17	31.8	ND	0	<0.02	<0.02		2.6	-9.1
PL	02.04.2016	33.2	6.42	<sup>b</sup> 22.2	7.88	195	3200	93.3	1810	225	60.1	10	440	<0.1	0.05	<0.02	<0.02	1.3	0.4	1.5
S5	05.2015	30	5.2	25.7	4.9	11.3	17700	365	8950	1060	318	25.3	2610	<0.1	0.9	0.12	0.23	-9.9	-4.8	-5.5
S6	05.04.2016	28.2	7.24	<sup>b</sup> 22.2	11.5	337	18700	426	11000	1320	372	1.21	2590	<0.1	0.31	ND	0.08	5.0	2.6	2.7

ND – not detected; Lowest standard used for Cs=0.10 ppm; Fe=0.05 ppm; Rb=0.02/0.05 ppm; Li=0.02 ppm; B=1.00 ppm; a – Analytical method not applicable to acidic sample; b – pH taken at 19.2-25.2°C and not reported per sample therefore a middle value was used for all the samples; c – charge balance from WATCH; d – charge balance from Powell and Cumming 2010 sheet; e – percent error from PHREEQC

SH5 – Sisip hot spring 2015; SH6 – Sisip hot spring 2016; MrH – Mararag hot spring; CtH – Cabattowan hot spring; McH – Magasasuc hot spring; CW – Coneig warm spring; SW – Sisip warm spring; NW – Naguilian warm spring; SC – Sisip cold spring; BC – Balatubat cold well; McL – Magasasuc Lake; PL – Pamoctan Lake; S5 – seawater 2015; S6 – seawater 2016

Samples with charge balance above 5% are highlighted in red in while samples with charge balance below 5% are highlighted in black

For the cold groundwater samples, SC and BC, the sampling temperatures were 26.7°C and 30°C. The waters are characterized by neutral pH of 7.07 and 7.29, respectively. Silica concentrations are slightly elevated ranging from 73.7 to 93.7 ppm while B is at 1.22 ppm. For both, HCO<sub>3</sub> is comparable with concentrations of 94.5 and 99.4 ppm. Higher SO<sub>4</sub> concentration of 114 ppm was measured in SC while BC has only 6.72 ppm. The Sisip cold spring (SC) is located on the southwest flank of Mt. Camiguin de Babuyan, near the Sisip hot and warm springs (SH, SW).

The thermal manifestations have temperatures of 39.9-90°C. Two hot springs, SH and MrH, have an acidic pH of 1.53-2.57. The remaining thermal waters are near neutral to slightly basic, 6.98-8.76. SiO<sub>2</sub> concentrations are relatively varied. The three warm springs (CW, SW, NW) and two hot springs (MrH and McH) have SiO<sub>2</sub> concentrations near groundwater values at 68.9-107 ppm. The SH has elevated values of 181-184 ppm while CtH has the highest concentration equal to 259 ppm. The dominant cation is Na, with some thermal waters having elevated values of Ca and Mg and one hot spring (McH) with a higher K concentration. The anions are mainly Cl and SO<sub>4</sub> except for two warm springs, CW, and SW, where HCO<sub>3</sub> is the major anion.

#### 4.1.2 Water classification

Based on the classification of geothermal waters by Ellis and Mahon (1977), the samples were classified into four groups according to the percentage of major ion concentrations in ppm. These groups are the alkali-chloride waters, acid sulphate waters, acid sulphate-chloride waters and bicarbonate waters.

Two hot springs were identified as alkali-chloride springs, that is McH and CtH. The McH has the highest Cl concentration reaching up to 5510 ppm as well as the highest Na concentration with 3130 ppm, K was measured 209 ppm, Ca 416 ppm and Mg 267 ppm. The second hot spring is CtH with Cl of 733 ppm and Na of 482 ppm.

Under the acid sulphate-chloride waters are MrH and SH5/6. Both are acidic and analysis for HCO<sub>3</sub> are not available for these samples. The SH5/6 have higher Cl of 1870-2100 ppm and almost the same amount of SO<sub>4</sub> from 1780 to 1860 ppm. The MrH on the other hand has higher Cl (2390 ppm) compared to SO<sub>4</sub> (617 ppm). Major cations in both samples are Na with concentrations ranging from 931 to 1310 ppm, Ca with 143-224 ppm and Mg with 84.9-130 ppm. The SH5/6 is located near a solfatara and MrH is located northwest of the solfatara. The oxidation of H<sub>2</sub>S to SO<sub>4</sub> and surface rock dissolution might have affected the composition of these waters. Thus, MrH, SH5 and SH6 are not suitable for prediction of subsurface properties.

The CW and SW are identified as bicarbonate waters with HCO<sub>3</sub> of 158 ppm and 116 ppm, respectively. Na is the major cation in both waters ranging from 59.2 to 61.5 ppm. These waters may be derived from CO<sub>2</sub> rich steam condensing or mixing with ground or surface water and are commonly found on the peripheries of geothermal systems. These waters may be used to predict subsurface properties if appropriate mixing models are used (Arnórsson, 2000).

The major anion for NW is SO<sub>4</sub> with 127 ppm and major cations are Na and Ca with concentrations of 53 ppm and 41.6 ppm, respectively. This water has a neutral pH of 6.98 so it cannot be considered an acid sulphate water.

Giggenbach (1991) also developed a way to classify geothermal waters using the chloride-sulphate-bicarbonate ternary diagram. The Cl-SO<sub>4</sub>-HCO<sub>3</sub> diagram, shown in Figure 6, classifies the water based on the major anions present in the sample. The sample nearest to the HCO<sub>3</sub> apex is BC, followed by CW and SW, and therefore these samples can be classified as peripheral waters that might have interacted with surface waters. They do not represent the deep geothermal fluid. The CW has elevated Cl concentration while SW has both high Cl and SO<sub>4</sub>. The NW and SC are plotted in the steam heated waters with around 40-50% SO<sub>4</sub>.

The group best suited for interpreting the deep fluid processes is comprised of neutral, low  $\text{SO}_4$ , high Cl “geothermal waters” along the Cl- $\text{HCO}_3$  axis or close to the Cl corner. The seawater (S5, S6) and lake waters (McL, PL) plot near the Cl apex reflecting higher Cl content due to the seawater contribution. The thermal sample closest to the mature water’s region is McH and due to its chemical similarity to PL indicates that its Cl content may come from other sources aside from geothermal fluid. Along the Cl- $\text{SO}_4$  axis are MrH, SH5 and SH6. CtH has more than 50% of Cl and more than 20% of  $\text{SO}_4$  and  $\text{HCO}_3$  indicating that it is a mixed water that could originate from the deep geothermal fluid but also has been subjected to surface processes.

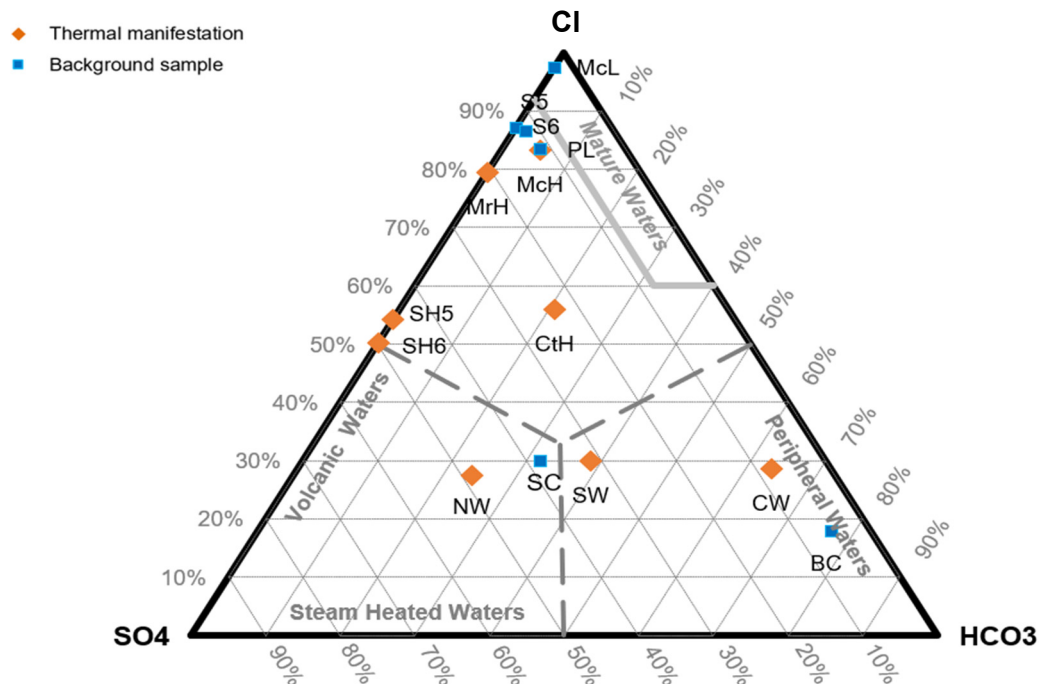


FIGURE 6: Cl- $\text{SO}_4$ - $\text{HCO}_3$  water classification ternary diagram showing the water samples of the Camiguin de Babuyan Geothermal Field. H-hot spring, W-warm spring, C-cold spring, S-seawater, L-lake

## 4.2 Geothermometry

With the  $\text{Na}/1000\text{-K}/100\text{-Mg}^{0.5}$  ternary diagram, Giggenbach (1988) provided an approach to differentiate which samples are in equilibrium with Na-K-Mg containing minerals. As shown in Figure 7, all the spring samples are classified as immature waters suggesting mixing with near surface water. Thus, these waters cannot be used to determine subsurface temperature or should be treated with caution when used in geothermometry. The nearest samples to partial equilibration are McH and MrH. The samples nearest to the Mg apex are CtH and NW, suggesting an uptake of Mg during ascent and discharge. High Mg mobility is common in low-temperature waters (e.g., Arnórsson, 2000).

All thermal waters were used for calculating the cation and silica geothermometry with the aid of the liquid analysis spreadsheet (Powell and Cumming, 2010). In Table 3 the results of these calculations are presented. The subsurface water temperature ranges from 89-199°C obtained by silica geothermometers, and 90-284°C assessed with Na/K geothermometry.

The temperatures calculated by the geothermometers in WATCH (Table 4) were like the ones assessed using the liquid analysis spreadsheet (Powell and Cumming 2010, Table 3). Silica geothermometry calculations give a temperature ranging from 89 to 186°C whereas Na/K geothermometers give higher temperature ranging from 136 to 277°C.

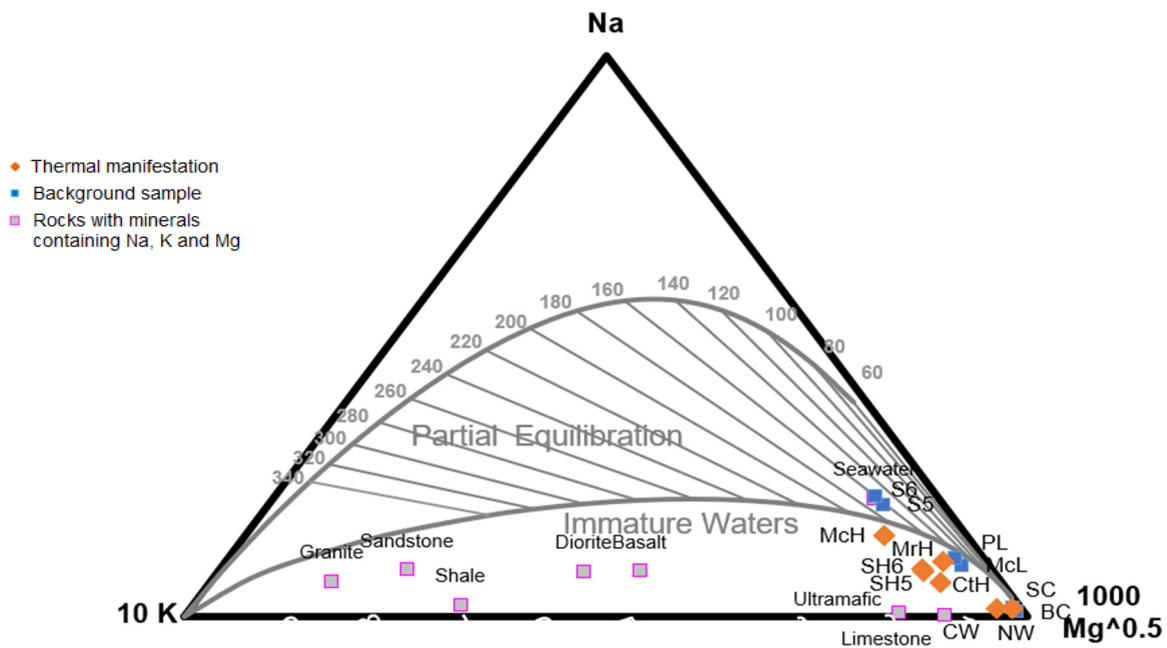


FIGURE 7: Na-K-Mg<sup>0.5</sup> triangular diagram showing the samples of the Camiguin de Babuyananes Geothermal Field. H-hot spring, W-warm spring, C-cold spring, S-seawater, L-lake

TABLE 3: Geothermometers calculated for all thermal springs using the liquid analysis spreadsheet ver. 3 by Powell and Cumming (2010). The temperatures are given in °C

ID	Chalcedony <sup>a</sup>	Quartz <sup>b</sup>	Quartz adiabatic <sup>c</sup>	Na-K-Ca <sup>c</sup>	Na/K <sup>d</sup>	Na/K <sup>e</sup>	Na/K <sup>f</sup>	Na/K <sup>g</sup>
SH5	152	175	163	190	216	186	232	194
SH6	151	174	162	190	218	188	233	196
MrH	89	117	115	165	167	126	185	137
CtH	180	199	183	198	232	206	246	213
MsH	98	126	123	184	185	148	202	157
CW	109	137	132	90	284	276	294	278
SW	114	141	135	186	186	150	204	159
NW	111	138	133	196	196	161	213	170

<sup>a</sup>conductive model, Fournier (1989); <sup>b</sup>conductive model, Fournier and Potter (1982); <sup>c</sup>Fournier (1981); <sup>d</sup>Fournier (1979); <sup>e</sup>Truesdell (1976); <sup>f</sup>Giggenbach (1988); <sup>g</sup>Arnórsson (1983)

TABLE 4: Geothermometers calculated for all thermal springs using WATCH (Arnórsson et al. 1982, Bjarnason 2010). The temperatures from the chalcedony (boiled model) geothermometer of five samples were considered the most probable temperatures of the reservoir (highlighted). The temperatures are given in °C

Sample ID	Chalcedony cooled	Chalcedony boiled	Quartz cooled	Quartz boiled	Na/K cooled	Na/K boiled
SH5	152.4	144.4	166	166	197.7	198.1
SH6	151.1	143.3	165.1	165.1	200.8	201.2
MrH	88.7	86.5	116.1	116.1	136.1	136.3
CtH	172.7	166.6	180	186.1	214.7	216
McH	96.9	97.1	122.2	123.9	157	157.4
CW	103.1	102.9	127	133.3	275.3	277.2
SW	113.5	107	135.7	137.1	162.3	162.9
NW	110.3	104.1	133.2	134.2	173.5	174.8

Because of disequilibrium between the waters and Na-K-Mg containing minerals, none of the samples were representative of the deep geothermal fluid and it is likely that the calculated temperature is not the temperature of the deep reservoir fluid. Moreover, due to the disequilibrium between the Na/K containing minerals and the deep fluid, the Na/K geothermometers are probably not suitable. Quartz geothermometers give temperatures below 150-180°C for most of the samples, however, this geothermometer is more accurate above these temperatures. The most suitable geothermometer therefore for this area is chalcedony, which is accurate for temperatures below 150-180°C (Arnórsson, 2000). Note that SH5, SH6, and MrH have acidic pH and therefore their calculated temperatures may not be accurate as silica and cation geothermometers are not applicable for acidic fluids (Arnórsson et al., 1983; Fournier, 1979; Giggenback, 1988). Thus, only the temperatures from chalcedony (boiled model) geothermometer of five samples were considered as the current probable temperatures of the reservoir. The calculated temperature ranges from 97.1 to 167°C. The highest temperature was calculated from CtH, which is on the west flank of Mt. Camiguin Volcano. The McH has the highest Cl concentration, however, it gives the lowest temperature which is 97°C. This sample is located far from the volcano, towards the northwest. The CW is a peripheral water located towards the north of the volcano.

### 4.3 Mineral saturation state

Summarized in Table 5 are the minerals that saturation states in the sampled waters were calculated for at the chalcedony temperature (Table 4). Most of the samples show supersaturation with respect to calcite, goethite, hematite, magnesite, diopside, forsterite, and magnetite. They are also close to equilibrium with respect to quartz and chalcedony. The deep geothermal fluid is undersaturated with minerals such as anhydrite, amorphous silica, and gypsum. It is also undersaturated with respect to high temperature minerals such as wollastonite, fayalite, forsterite, tremolite, and diopside.

TABLE 5: Mineral assemblages in the reservoir at the calculated reservoir temperatures

Sample ID	Mineral assemblage at reservoir temperature (SI > 0)	Minerals that will not form at reservoir temperature (SI < 0)
CtH	calcite, ferrite-Ca, ferrite-Mg, forsterite, goethite, hematite, magnesite, magnetite, quartz, tridymite	anhydrite, gypsum, halite, siderite, amorphous silica, wollastonite
McH	calcite, chrysotile, diopside, dolomite, goethite, hematite, magnetite, magnesite, quartz	anhydrite, coesite, alpha cristobalite, beta cristobalite, enstatite, fayalite, forsterite, gypsum, gyrolite, wollastonite, wurtzite, amorphous silica
CW	calcite, aragonite, chrysotile, dolomite, diopside, enstatite, forsterite, goethite, hematite, magnesite, magnetite, quartz, tremolite	amorphous silica, anhydrite, chalcedony, coesite, alpha cristobalite, beta cristobalite, fayalite, gypsum, halite, siderite, wollastonite
SW	chalcedony, quartz	calcite, amorphous silica, anhydrite, aragonite, chrysotile, coesite, alpha cristobalite, beta cristobalite, dolomite, diopside, enstatite, forsterite, gypsum, halite, magnesite, periclase, tremolite, tridymite, wollastonite

The relation between the log Q/K of amorphous silica, anhydrite, calcite, chalcedony and quartz and temperature (Figure 8) was also investigated to anticipate the behaviour of the waters with respect to these minerals at various temperatures. The temperatures chosen for this study is arbitrary. The highest temperature was chosen in consideration with the temperatures given by silica and cation geothermometers while the lowest temperature is based near the sampling temperatures though it is understood that water less than 100°C does not boil at sea level.

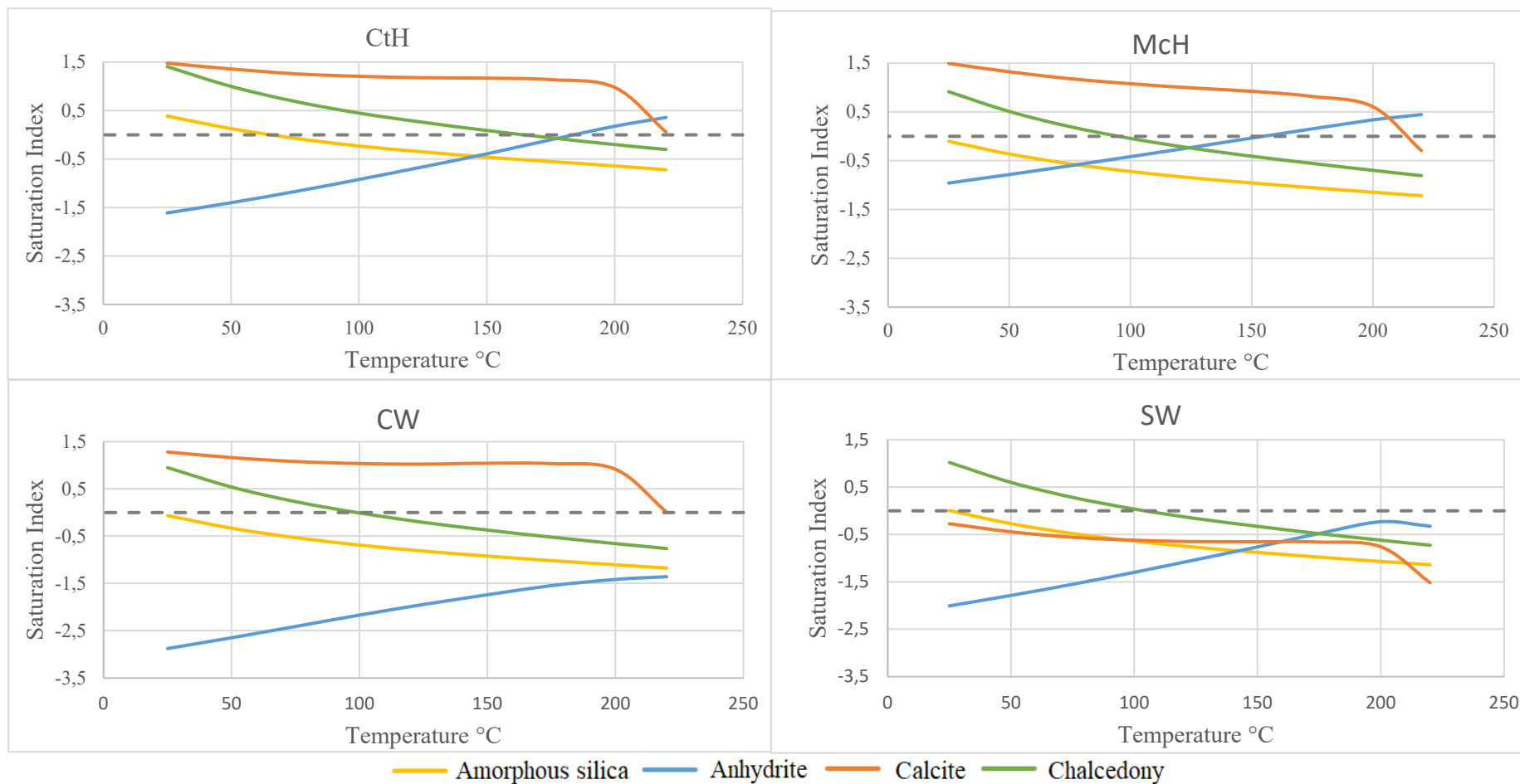


FIGURE 8: Mineral saturation indices of geothermal waters (CtH, McH, CW and SW) with respect to amorphous silica, anhydrite, calcite, and chalcedony as a function of temperature

The adiabatic boiling model calculations from 220°C to 25°C shows that calcite might precipitate when waters are cooled to ambient temperature. Amorphous silica might precipitate at lower temperature from the CtH water. Anhydrite will also precipitate above the calculated reservoir temperature.

#### 4.4 Mixing

The Cl and B are conservative constituents in geothermal fluids (Arnorsson, 2000). Conservative elements remain in the fluids once they are added to the fluids, and therefore, they can be used to trace the origin and flow of geothermal fluids as these elements rarely precipitate from the waters at low to medium temperatures (Arnorsson, 2000). The samples were plotted (Figure 9) to see the behaviour of these elements. The two endmembers for the plot are groundwater (SC) and seawater (S5/S6). A linear relationship was observed for the thermal waters indicating mixing of hot and cold water. The McH has the highest Cl content like the Cl content at Sandawa Collapse of Mt. Apo geothermal reservoir (Alincastré, 2000) and MG-3D of Mahanagdong Sector of Tongonan geothermal field (Balmes, 1994). However, the linear trend towards the seawater (Figure 9) may signify mixing due to its location next to the coast (Figure 2) and for having the closest composition to that of seawater. If considering only the Cl content, approximately 29% of McH would be seawater. On the other hand, the proximity of SW to that of the groundwater endmember implies mixing of the geothermal fluid with cold groundwater rather than with seawater. The SH5, SH6, MrH and CtH are in between the two endmembers, indicating variable amounts of hot and cold influxes in its composition.

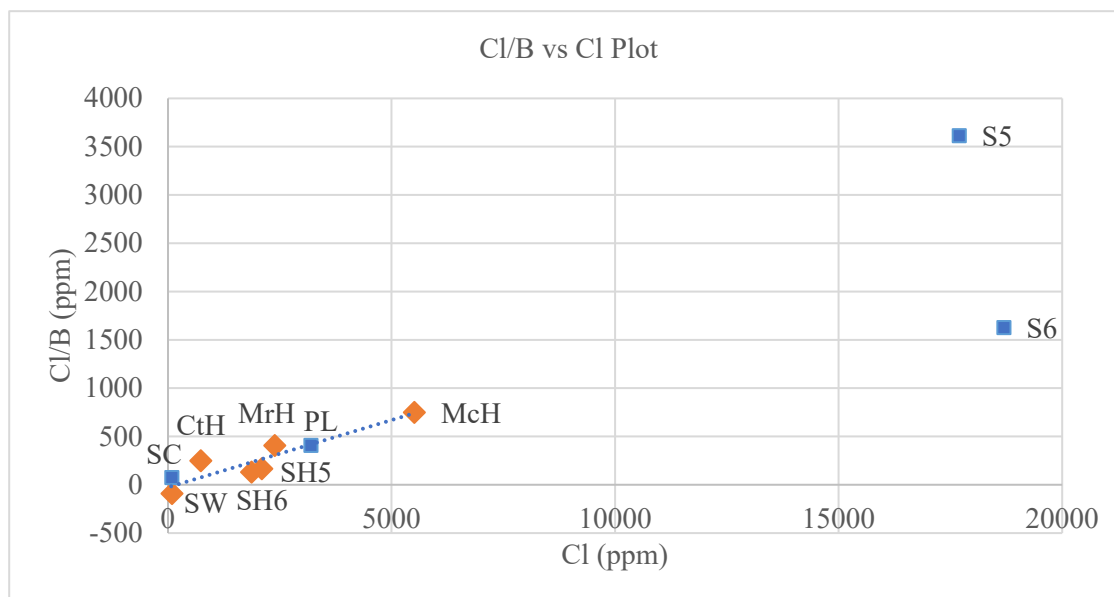


FIGURE 9: The Cl vs Cl/B plot of thermal waters (orange diamonds) and background samples (blue squares) from Camiguin de Babuyan

## 5. IMPLICATIONS FOR GEOTHERMAL UTILIZATION

Based on the chalcedony temperature, the most likely temperature in the subsurface is 97-167°C. The hottest spot in the prospect area is CtH on the northeastern part of Mt. Camiguin. All the investigated waters are possibly a mixture of seawater (S5, S6) or groundwater (SC) with a hotter geothermal fluid that exists deeper in the subsurface. The waters are generally neutral with acidic waters on the western flank of the volcano on top of the solfatara. The utilization of the fluids depends on the location of the area. Towards the north, west and northwest of the study area, the temperatures are calculated to be at around 100°C which is suitable for industrial uses like drying (Figure 10). On the west of Mt. Camiguin, the temperatures based on the chalcedony geothermometer can reach up to 167°C, which would have

an estimated enthalpy at 706 kJ/kg using the steam tables. This means the water can be used for binary power generation and industrial uses such as refrigeration and icemaking, fabric drying, lumber drying, cement and aggregate drying and drying of food products.

Corrosion of surface equipment due to the presence of acidic fluids were experienced in other geothermal fields in the Philippines (e.g., Bacon-Manito) (Martinez-Olivar et al., 2005), Mahanagdong (Angcoy and Arnórsson, 2015), and Apo (Los Baños et al., 2010)). Based on the fluid compositions from SH5, SH6 and MrH, corrosion would likely occur if the waters from the western side of the volcano would be utilized. Due to this area's extremely high acidity ( $\sim$ pH 2), it is recommended that these fluids are not utilized until new technology has been developed for the utilization of acidic fluids (Sanada et al. 2000).

The calculated fluid in McH on the north-northwest of the volcano shows an increased salinity (up to approximately 5000 ppm). Thus, possible corrosion or scaling from geothermal fluid mixing with seawater could occur (Conover et al., 1979; Opondo, 2002), and further investigation would be recommended before utilization.

Both calcite and anhydrite (at higher temperatures) show supersaturation during cooling (Figure 8). These minerals might precipitate during the utilization of the waters. On the other hand, amorphous silica, which is considered one of the most common scaling minerals, is not anticipated to precipitate during utilization.

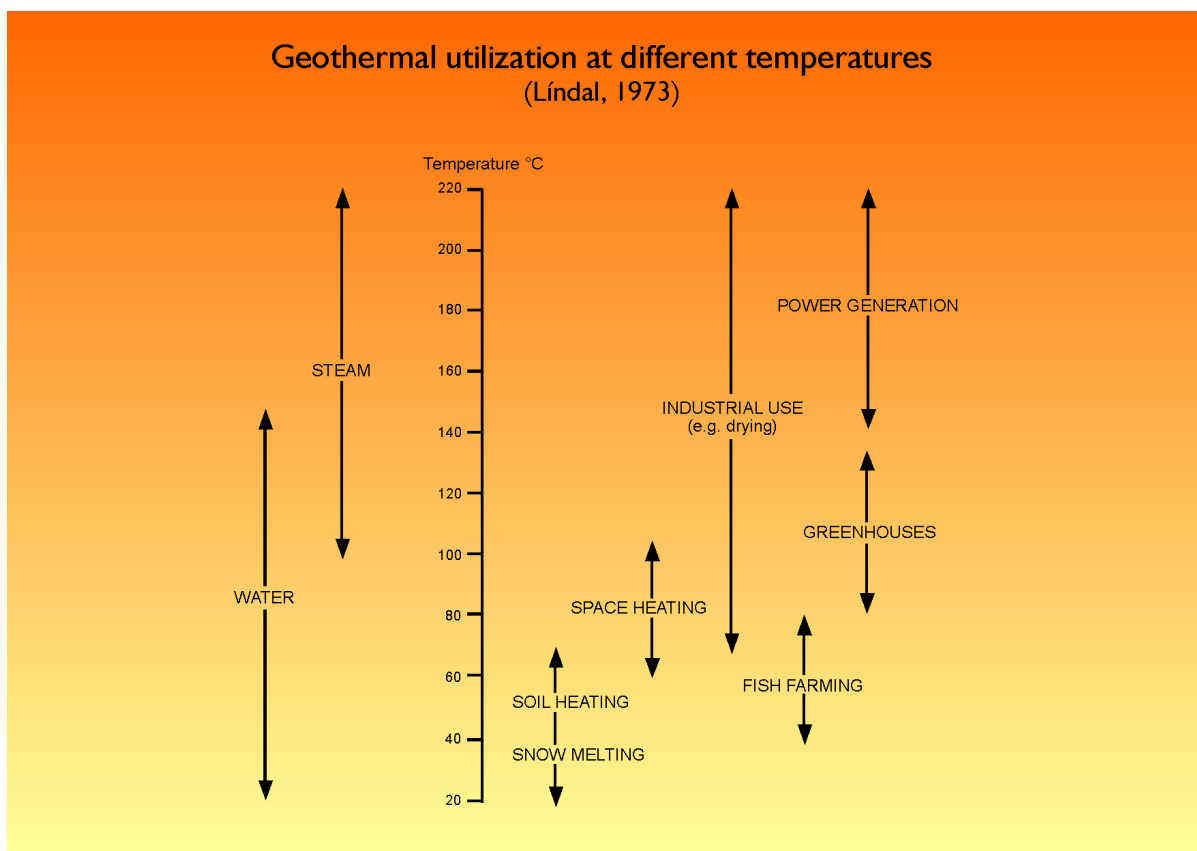


FIGURE 10: Líndal (1973) diagram showing the different types of utilization depending on temperature

## 6. CONCLUSIONS

Several conclusions can be drawn from this study of thermal waters in the Camiguin Geothermal Field.

- The calculated subsurface temperature is 97-167°C (intermediate temperature) with an estimated enthalpy of 706 kJ/kg.
- The highest temperatures (150-167°C) are located closest to Mt. Camiguin de Babuyan, and 97-107°C to the western and northern side of the volcano.
- There is no representative geothermal fluid.
- The waters represent alkali-chloride, sulphate-chloride, and bicarbonate waters.
- The waters are suitable for geothermal utilization including binary power generation.
- Corrosion from acidic fluids on the west of the Mt. Camiguin and possible corrosion due to seawater on the north-northwest of the volcano will require further studies if utilization on these areas should be considered.
- The saturation state of the water suggests calcite, amorphous silica (lower T), and anhydrite (higher T) precipitation during cooling of the waters from reservoir to ambient temperatures.

## ACKNOWLEDGEMENTS

I cannot say thank you enough to the people who made it possible for me to attend the training programme and to write this paper. Here's my appreciation.

To the government of Iceland for awarding this fellowship through the GRO Training Programme under the dedicated and esteemed staff of Dr. Gudni Axelsson (Director), Mr. Ingimar G. Haraldsson (Deputy Director), Dr. Vigdis Harðardóttir (Operations Manager) for her patience and inputs on this paper, Mr. Markus A. G. Wilde (Programme Assistant) and especially to Ms. Málfríður Ómarsdóttir (Project Manager) who provided me with her support throughout the duration of the training leaving me a feeling I have a mother in Iceland.

To the management and staff of the Geothermal Energy Management Division for extending technical and personal support in the various stages of the study. To Mr. Ariel D. Fronda and Mr. Rainier Halcon, thank you so much for allowing me to attend this training. It has helped in a lot of ways, professionally and personally, and I will apply all my learnings to contribute to our dearest division. Special thanks to my colleagues/friends (you know who you are!) who asked me for a monthly meeting to update me and to provide support like additional data every time I needed it.

To all my professors in the geochemistry specialization, to Dr. Andri Stefánsson and Mr. Finnbogi Óskarsson, I learned a lot from you while enjoying my introduction to geochemistry.

To family, friends and loved ones, to my special person, we did it, and to the people who inspired me throughout the training, thank you.

Finally, to my supervisors, who I think are the greatest supervisors I ever had, Dr. Deirdre Clark and Dr. Iwona Galeczka, thank you for all the technical inputs, ideas, discussions, and inspirational emails you sent me. I could not have finished this paper without you. I felt kindness, warmth, so much patience and enough pressure from you, altogether these things made you the greatest.

## REFERENCES

- Alicanstre, R.S, Sambrano, B.M.G., Nogara, J.B., 2000: Geochemical evaluation of the reservoir response to exploitation of the Mindanao-1 Geothermal Production Field, Philippines. *Proceedings World Geothermal Congress 2000, Kyushu-Tohoku, Japan*, 2483-2488.
- Angcoy, E.C., and Arnórsson S., 2015: Systematics of rare alkalis and halogens in the high-temperature Mahanagdong Geothermal Field, Leyte, Philippines. *Proceedings World Geothermal Congress 2015, Melbourne, Australia*, 19-25.
- Arnórsson, S., Sigurdsson, S., and Svavarsson, H., 1982: The chemistry of geothermal waters in Iceland. I. Calculations of aqueous speciation from 0° to 370°C. *Geochim. Cosmochim. Acta*, 46, 1513-1532.
- Arnórsson, S., Gunnlaugsson, E., and Svavarsson, H., 1983: The chemistry of geothermal waters in Iceland III. Chemical geothermometry in geothermal investigations. *Geochim. Cosmochim. Acta*, 47, 567-577.
- Arnórsson, S. (ed.), 2000: *Isotopic and chemical techniques in geothermal exploration, development and use. Sampling methods, data handling, interpretation*. International Atomic Energy Agency, Vienna, 351 pp.
- Arnosson, S., Stefansson, A., Bjarnason, J.O., 2007: Fluid-fluid Interactions in Geothermal Systems. *Reviews in Mineralogy and Geochemistry* 65, 259-312.
- Balmes, C.P., 1994: The geochemistry of the Mahanagdong Sector, Tongonan Geothermal Field, Philippines. Report 2 in: *Geothermal Training in Iceland 1994*. UNU-GTP, Iceland, 31-52.
- Becker, G.B., 1901: *Geology of the Philippine Islands*. Washington Government Printing Office, Washington D.C., USA, 139 pp.
- Bjarnason, J.Ö., 2010: *The chemical speciation program WATCH, version 2.4*. ÍSOR – Iceland GeoSurvey, Reykjavik, website: [www.geothermal.is/software](http://www.geothermal.is/software).
- Camiguin de Babuyanes, 2011: *Archived at the Wayback Machine*, website: [https://web.archive.org/web/20110901184213/http://volcano.phivolcs.dost.gov.ph/update\\_VMEPD/Volcano/VolcanoList/camiguindebabuyanes.htm](https://web.archive.org/web/20110901184213/http://volcano.phivolcs.dost.gov.ph/update_VMEPD/Volcano/VolcanoList/camiguindebabuyanes.htm)
- Conover, M., Ellis, P., and Curzon, A., 1979: Material selection guidelines for geothermal power systems –An overview. In: Casper, L.A., and Pinchback, T.R., (eds.), *Geothermal scaling and corrosion*. ASTM, STP 717, 17 pp.
- Defant M., Jacques D., DeBoer J. and Joron J.L, 1989: Geochemistry and Tectonic Setting of the Luzon Arc, Philippines. *Geological Society of America Bulletin* 101, 663-672.
- Defant, M., Maury, R., Joron, J., Feigenson, M., Leterrier, J., Bellon, H., Jacques, D., and Richard, M., 1990: The geochemistry and tectonic setting of the northern section of the Luzon arc (the Philippines and Taiwan). *Tectonophysics*, 183, 187-205.
- Department of Energy, 2017: *First stage exploration of Camiguin de Babuyanes geothermal prospect integrated geoscientific assessment*. Philippines Department of Energy, unpublished internal report.
- Ellis, A.J., and Mahon, W.A.J., 1977: *Chemistry and geothermal systems*. Academic Press, New York, 392 pp.

- Fournier, R.O., 1977: Chemical geothermometers and mixing model for geothermal systems. *Geothermics*, 5, 41-50.
- Fournier, R.O., 1979: A revised equation for Na-K geothermometer. *Geoth. Res. Council, Trans.*, 3, 221-224.
- Fournier, R.O., 1981: Application of water geochemistry to geothermal exploration and reservoir engineering. *Geothermal Systems: Principles and Case Histories*, Ryback and Muffler eds., John Wiley and Sons NY, 109-143.
- Fournier, R.O., and Potter, R.W. II, 1982: A revised and expanded silica (quartz) geothermometer. *Geoth. Res. Council Bull.*, 11-10, 3-12.
- Fournier, R.O., 1989: Lectures on geochemical interpretation of hydrothermal waters. *UNU Geothermal Training Programme, Reykjavik, Iceland, Report 10*. [www.unugtp.is/solofile/33667](http://www.unugtp.is/solofile/33667)  
[www.unugtp.is/solofile/33668](http://www.unugtp.is/solofile/33668).
- Fronza, A.D., Lazaro, V.S., Halcon, R.M., and Reyes, R.G., 2021: Geothermal Energy Development: The Philippines Country Update. *Proceedings of the World Geothermal Congress 2020+1, Reykjavik, Iceland*, 8 pp.
- Giggenbach, W.F., 1988: Geothermal solute equilibria. Derivation of Na-K-Mg-Ca geothermometers. *Geochim. Cosmochim. Acta*, 52, 2749-2765.
- Giggenbach, W.F., 1991: Chemical techniques in geothermal exploration. In: D'Amore, F. (coordinator), *Application of geochemistry in geothermal reservoir development*. UNITAR/UNDP publication, Rome, 119-144.
- Hsieh, Y.H., Liu, C.S., Suppe, J., Byrne, T. B., and Lallemand, S., 2020: The Chimei submarine canyon and fan: A record of Taiwan arc-continent collision on the rapidly deforming overriding plate. *Tectonics*, 39, e2020TC006148.
- Huang, C-Y., Yuan, P.B., Tsao, S-J, 2006: Temporal and spatial records of active arc-continent collision in Taiwan: A synthesis. *Geological Society of America Bulletin*, 118, no.3/4, 274-288.
- Lallemand, S., 2016: Philippine Sea Plate inception, evolution, and consumption with special emphasis on the early stages of Izu-Bonin-Mariana subduction. *Progress in Earth and Planetary Science*, 3, 1-27.
- Los Baños, C.F., Rigor, D.M., Layugan, D.B. and Bayrante, L.F., 2010: The resistivity model of the Mindanao Geothermal Project, South Central Mindanao, Philippines. *Proceedings of the World Geothermal Congress 2010, Bali, Indonesia*, 6 pp.
- Lindal, B., 1973: Industrial and other applications of geothermal energy. *Geothermal Energy, Paris, UNESCO, LC No. 7297 138*, 135-148.
- Martinez-Olivar, M.V.M, See, F.S. and Solis, R., 2005: Isotopic response to changes in the reservoir in Bacman Geothermal Production Field, Philippines. *Proceedings of the World Geothermal Congress 2005, Antalya, Turkey*, 7 pp.
- McDermott, F., Delam, M.J., Hawkesworth, C.J., Maury, R.C., and Jorom J.L., 1993: Isotope and trace element evidence for three component mixing in the genesis of the North Luzon arc lavas (Philippines). *Contrib. Mineral. Petrol.* 113:9, 23.

Nieva, D., and Nieva, R., 1987: Developments in geothermal energy in Mexico, part 12-A: Cationic composition geothermometer for prospection of geothermal resources. *Heat Recovery Systems and CHP*, 7, 243-258.

Opondo, K.M., 2002: Corrosion tests in cooling circuit water at Olkaria I Plant and scale predictions for Olkaria and Reykjanes Fluids. Report 10 in: *Geothermal Training in Iceland 2002*. UNU-GTP, Iceland, 147-186.

Parkhurst, D.L., and Appelo, C.A.J., 2013: *Description of input and examples for PHREEQC (vs. 3) - A computer program for speciation, batch-reaction, one-dimensional transport, and inverse geochemical calculations*. US Geological Survey, Techniques and Methods, Book 6, A43, 497 pp.

Peña, R., and Aurelio, M., 2010: *Geology of the Philippines, 2<sup>nd</sup> edition*. Mines and Geosciences Bureau, Philippines, 532pp.

PHIVOLCS, 1997. *Catalogue of Philippine Volcanoes, vol. 1, Active Volcanoes (revised from 1994 version)*, unpublished.

Powell, T., and Cumming, W., 2010: Spreadsheets for geothermal water and gas geochemistry. *Proceedings of the 35<sup>th</sup> Workshop on Geothermal Reservoir Engineering, Stanford University, Stanford, CA*, 10 pp.

Reed, M.H., and Spycher, N.F., 1984: Calculation of pH and mineral equilibria in hydrothermal water with application to geothermometry and studies of boiling and dilution. *Geochim. Cosmochim. Acta*, 48, 1479-1490.

Richard M., Maury, R.C., Bellon, H., Stephan, J.F., Boirat, J.M., and Calderon, A., 1986: Geology of Mt. Iraya volcano and Bahm island, northern Philippines. *Philipp. J. Volcanol.* 3, 1-27.

Sanada, N., Kurata, Y., Nanjo, H., Kim, H., and Ikeuchi, J., 2000: IEA deep geothermal resources subtask C: Materials, progress with a database for materials performance in deep and acidic geothermal wells. *Proceedings of the World Geothermal Congress 2000, Kyushu-Tohoku, Japan*, 2411-2416.

Tonani, F., 1980: Some remarks on the application of geochemical techniques in geothermal exploration. *Proceedings, Adv. Eur. Geoth. Res., 2<sup>nd</sup> Symposium, Strasbourg*, 428-443.

Truesdell, A.H., 1976: Geochemical techniques in exploration (Summary of Section III). *Proceedings of the 2<sup>nd</sup> United Nations Symposium on the Development and Use of Geothermal Resources, San Francisco, CA, USA*, 1, 53-79.

Voigt, M., Marieni, C., Clark, D.E., Gíslason, S.R., Oelkers, E.H., 2018. Evaluation and refinement of thermodynamic databases for mineral carbonation. *Energy Procedia*, 146, 81-91.

Yang, T., Lee, T., Chen, C., Cheng, S., Knittel, U., Punongbayan, R., and Rasdas, A., 1996: A double island arc between Taiwan and Luzon: consequence of ridge subduction. *Tectonophysics*, 258, 85-101.

## APPENDIX I - REGIONAL GEOLOGIC SETTING

### 1. Tectonic setting

Camiguin de Babuyanes (CDB) is a stratovolcano located on the southwest of Camiguin Island, Calayan, Cagayan, Philippines. It is classified as an active volcano by the Philippine Institute of Volcanology and Seismology. One historical eruption was recorded in 1857 (Camiguin de Babuyanes, 2011) The stratovolcano is now in solfataric stage (Becker, 1901).

The CDB belongs to the Babuyan Islands Group (Peña and Aurelio, 2010), in the northernmost part of the Philippines which is a part of the southernmost portion of Babuyan subprovince (Babuyan Segment of Defant et al. 1990, Bashi Segment of Yang et al. 1996), shown in Figure 12. The Babuyan subprovince is bounded by Huatung Basin, a >4,000 m deep practically closed basin (Hsieh et al, 2020) to the north-northeast. On the east, it is bounded by the Gagua Ridge, a 300 km long, 4 km high north-south trending ridge at 123° E separating the Huatung Basin and the West Philippine Basin (Lallemand, 2016). On the west, by the Hengchun Ridge, an accretionary prism formed by the subduction of South China Sea oceanic crust under the Philippine Sea Plate (Huang et al, 2006) through the Manila Trench. On the south, it is bounded by Luzon Island.

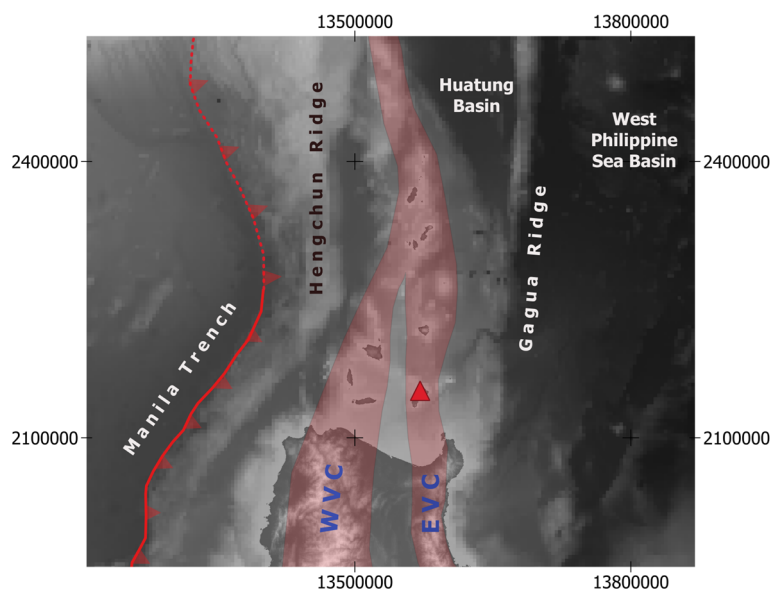


FIGURE 12: Regional tectonic setting of Camiguin de Babuyanes showing Mt. Camiguin (red triangle) along the EVC, bounded on the west by Hengchun Ridge, on the north-northeast by Huatung Basin, on the east by Gagua Ridge, and on the south by Luzon Island. Modified from Yang et al. 1996

Two volcanic chains can be observed within this subprovince – the western volcanic chain (WVC) and the eastern volcanic chain (EVC). There was no reported active volcanism in WVC while 5 out of 13 volcanoes/volcanic islands are still active in EVC. Based on whole rock K-Ar age taken from fresh samples, magmatic activity in WVC ceased at 4-2 Ma while activity in EVC is mainly Pleistocene. The volcanic islands of WVC have also nearly flat relief and consists of partially to well-developed laterites and terraces while the volcanoes of the EVC have partially to well preserved volcanic cones with steep slopes. Another difference is that the EVC

lavas have an enriched signature in comparison to the WVC lavas at the same latitude (Yang et al., 1996)

It was proposed that these two chains are an expression of a double arc structure. The WVC was formed like a typical intra-oceanic arc. Then, when the extinct ridge of South China Sea, the Scarborough Seamount Chain reached the subduction zone, it resisted subduction, so arc magmatism stopped at this intersection. Meanwhile the northern part of the Taiwan-Luzon Arc was also colliding with the Eurasian Plate forming Taiwan and ending the volcanism at the northern end of the Babuyan subprovince. The resistance of the ridge to subduct caused part of the ridge complex to transfer to the upper plate. When the strength of the subduction increased, it forced the ridge to resume subduction. The Scarborough Seamount Chain has greater buoyancy than the subducting South China Sea plate because of its low

density young and thick ridge. Because of this buoyancy, the subduction angle decreased in the location where the ridge is subducting, breaking the subducting plate near the boundary between the Eurasian Plate and South China Sea Plate, which is possibly the reason for the enriched signature found in the EVC lavas. This resulted to an active volcanism forming the EVC. (Yang et al., 1996)

## 2. Regional geology

The EVC is composed of Batan (Mt. Iraya), Babuyan, Didicas, Camiguin, Mt. Cagua, Y'Ami, North, Mabudis, Siayan, Diogo, Balintang, Hsiaolanyu, and Lutao. Most of the volcanic rocks in this chain that has an age of approximately 1 Ma or less are basaltic andesites with minor basalts and andesites (McDermott et al., 1993). The lithology of most of these volcanic islands are described below.

The oldest rocks can be found on Batan Island. These are weathered flows consisting of hornblende and orthopyroxene-bearing andesites. The age of these flows is Late Miocene (9-7 Ma). These occur occasionally below the reefal limestones and young ash deposits of Mt. Iraya, on the north of Batan Island. On the south, the Pliocene Matarem composite volcano, with deposits dating from 5.8-1.7 Ma, is composed of several andesitic necks and plugs, andesite flows and younger basaltic flows with minor associated pyroclastics. These lavas are highly porphyritic and are composed of basalts to hornblende-orthopyroxene acid andesites. Reworked layer deposits with interbedded ash and pumice layers dominate the periphery of this volcano.

In the north, the Quaternary Mt. Iraya lavas range in composition from basaltic to andesitic. The basalts have xenocrysts of peridotitic xenoliths while the hornblende-bearing andesites have ultramafic xenoliths, such as deformed harburgites, dunites, and lherzolites. Lavas on the island older than 2 Ma are calc-alkaline while younger lavas are high-K calc-alkaline. A pyroclastic deposit, consisting of sequences of ash fall and pumice fall deposits, at the west foot of Mt. Iraya dates to 1,480 B.P. (Richard et al., 1986).

Calayan Island is composed of four effusive volcanic centers – Mt. Nongabaywaman, Mt. Macara, Mt. Calayan, and Mt. Piddan. These are composed of basaltic andesite (6-7 Ma), andesitic lava flows (5-6 Ma), and a rhyolitic lava flow (4 Ma) (Defant et al., 1989). Near the shore, these are overlain by Plio-Quaternary reef limestones.

Sabtang Island is composed of calc-alkaline basalt (Defant et al., 1990) and basaltic andesite with ages ranging from 3.8 to 2.9 Ma.

Babuyan de Claro Island has four volcanic centers – Cayonan, Naydi, Dionisio, Mt. Pangasun and Mt. Babuyan. These are composed of a succession of calc-alkaline andesitic and basaltic andesitic lava flows. The last recorded eruptions on the island were in 1831 and 1917 (PHIVOLCS, 1997).

Mt. Cagua is the youngest in the volcanic chain, dated to the Pleistocene. It is an active andesitic volcano intruding the Miocene sedimentary rocks southeast of Gonzaga, Cagayan. Solfataric activity was recorded in 1860 and 1907 (PHIVOLCS, 1997).